Forced convective heat transfer from premixed flames

—Part 1: Flame structure

G. K. Hargrave*†, M. Fairweather*† and J. K. Kilham*

In this, the first part of a two-part study of convective heat transfer from impinging flames, the aerodynamic structure of four flames was studied. The flames examined were of stoichiometric mixtures of methane and air with a Reynolds number range extending from the laminar to fully turbulent flow regimes. Instantaneous Schlieren photographs revealed that with increasing Reynolds number the flame reaction zone extended further downstream and became thicker and more diffuse. Associated with this, measurements of mean and rms velocities and mean temperatures showed that the properties of the flames became drawn out in the downstream direction as Reynolds number increased. Schlieren-stroboscopic techniques also revealed the existence of large scale vortex rings which originated in the shear layer of the flames, and which were found to cause low frequency oscillations in measured instantaneous velocities. These oscillations lead to misleadingly high levels of rms velocities downstream of the flame reaction zone which should not be interpreted as representing turbulence within the flame.

Keywords: *heat transfer, convection, flames, methane, aerodynamic structure*

Introduction

In conventional industrial furnaces heat transfer to the stock occurs mainly by thermal radiation from incandescent furnace walls which are heated by flames. In recent years, however, rapid heating techniques have become increasingly popular since they offer the possibility of saving energy and improving the quality of the hot product. One method of achieving rapid heating when using clean, high grade gaseous fuels is through the jet impingement technique, where convective heat transfer is maximized by impinging flames directly on the surface of the stock.

Impingement heat transfer from laminar, premixed gaseous fuel–air flames has received much attention, and early work by Kilham and coworkers[1-3] helped to elucidate the mechanisms by which energy is transferred from such flames to solid bodies. The use of oxygen-enriched air or oxygen as an oxidant in laminar, premixed flames has been studied[4-6] because of its potential for increasing flame temperatures and, hence, convective heat transfer rates. Electrically boosted flames have also been examined for the same reason[7,8]. Only in recent years has attention turned to a consideration of the extent to which turbulence in a free firing flame can affect heat transfer rates[9-12].

Free stream turbulence is known to augment the rate of convective heat transfer from nonreacting flows that impinge on solid bodies which generate large streamwise pressure gradients. This effect has been demonstrated experimentally for bodies placed in both turbulent wind tunnel flows[13,14] and turbulent air jets[15,16]. Turbulence enhancement of heat transfer rates has also been observed in combusting flows[11,12].

The present study examines impingement heat transfer from premixed methane–air flames over a wide range of burner exit Reynolds numbers and flame equivalence ratios. The range of Reynolds numbers employed was chosen to generate flames which extended from the laminar to fully turbulent flow regimes. Because the rate of impingement heating is intimately related to the aerodynamic structure of such flames the present study is reported in two parts. The first part considers the structure of four flames which span the Reynolds number range considered. Attention is restricted to the case of stoichiometric flames, although the results obtained are qualitatively representative of all the various equivalence ratio flames examined. The second part of the study considers impingement heat transfer to the stagnation point of a body of revolution (hemispherical-nosed cylinder) and a circular cylinder placed in the flames.

Experimental work

The initial part of the burner used in the present study consisted of a 700 mm length of 16 mm internal diameter copper tubing which provided a smoothing section to eliminate flow turbulence generated by the methane–air input port. The final 200 mm of the burner tube, shown in Fig 1, was constructed from brass tubing. This section of the burner provided a facility for the introduction of turbulence promoters or smoothing meshes by the use of a series of brass slip rings held inside a brass sleeve, although this facility was not used in deriving the results reported in the present work.

In order to provide flame stabilisation at all flow rates a hydrogen pilot flame was employed. This was generated by passing hydrogen through a 28 mm internal diameter copper pipe mounted concentrically with the burner axis and tapered to form a 1.5 mm wide annulus at the burner exit. In order to ensure that the pilot flame did not interfere with the premixed methane–air flames and thereby affect the structure of, and heat transfer from, these flames, laser Doppler anemometry (LDA) and heat transfer measurements were made in the methane–air flames for various hydrogen flow rates. It was found that a flow rate of only 20 $cm^3 min^{-1}$ provided flame stabilisation for the highest Reynolds number flow employed and did not affect the properties of the lowest Reynolds number flame.

Methane (with a purity of 99.9 vol%) and air were supplied to the burner through separate lines and were metered using rotameters. Methane was passed through a one-way valve and a

* Department of Fuel and Energy, The University, Leeds LS2 9JT, UK
† Present address: British Gas Corporation, Midlands Research Station, Wharf Lane, Solihull, West Midlands B91 2JW, UK. (Correspondence to Dr Fairweather at this address.)
Received 9 April 1986 and accepted for publication on 29 August 1986

0142-727X/87/010055-09$3.00

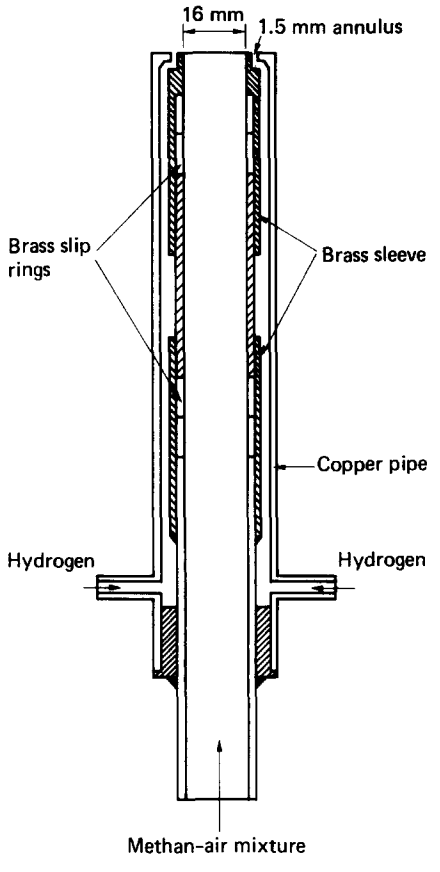

Figure 1 Schematic of the premixed methane–air burner

flame trap before being mixed with air at the burner inlet. The air line contained a seeding system to provide scattering centres for LDA measurements. Seeding was achieved using a fluidized bed cyclone device based on the design of Glass and Kennedy[17]. Air passing through this device was seeded with alumina particles with a mean size of 1 μm and a maximum size of 2 μm determined by electron micrography. The seeded air was then passed through a settling chamber to remove any large particles or agglomerates.

Laser Doppler anemometry was used for the measurement of velocities in the flames. The system employed was of the dual beam, forward scatter design and used a 2 W argon ion laser with a wavelength of 488 nm. Processing of the photomultiplier output was accomplished using the frequency tracking technique, and a microcomputer-controlled data acquisition sytem with a maximum sampling rate of 10 kHz was used for recording the raw data. The complete system described facilitated the direct measurement of mean velocites and the root mean squares (rms) of velocity fluctuations.

Temperatures within the flames were measured using uncoated platinum/platinum–13% rhodium thermocouples. The thermocouple junction was formed by butt-welding using a capacitor discharge device which produced junction diameter approximately equal to the 0.24 mm diameter wire employed. Measured temperatures were corrected for radiative heat losses from the thermocouple using an energy balance, based on the method described by Fristrom and Westenberg[18].

Results and discussion

Flame structure and impingement heat transfer measurements were obtained for mean flow Reynolds numbers of 2000, 4000, 8000 and 12 000 at the burner exit. This range of flows ensured the study of both laminar and fully turbulent flames. Premixed methane–air mixtures with equivalence ratios from 0.8 to 1.2 were also examined. Here, equivalence ratio is defined as the ratio of the stoichiometric amount of oxygen required to burn the fuel to CO_2 and H_2O to the actual amount used. As noted previously, the present paper restricts attention to stoichiometric flames at the four Reynolds numbers of interest. This group of flames was found to be representative of all the premixed flames studied.

General flame structure

Instantaneous Schlieren photographs of the four stoichiometric flames are shown in Fig 2. These photographs were obtained using an argon spark-jet light source which gave an illumination period of 0.2 μs. Under conditions of laminar flow at $Re = 2000$ (Fig 2(a)) a stable conical reaction zone is formed which appears as a sharp boundary between unburnt and burnt gas. The reaction zone of this flame is approximately 1 mm thick. Reynolds number flows of approximately 3000 and above give rise to fully developed turbulent flames which have an irregular wrinkled appearance. This is caused by turbulence generated in the burner pipe flow and is also due to the augmentation of turbulence by the combustion process itself. In the $Re = 4000$ flame (Fig 2(b)) the reaction zone is only moderately wrinkled close to the burner rim, but becomes increasingly ragged with distance downstream. The reaction zone of this flame is therefore much more diffuse and ill-defined than that of the $Re = 2000$ flame, and extends over a distance of approximately 16 mm on the burner axis. With increasing Reynolds number the reaction zone starts to wrinkle much closer to the burner rim, and becomes progressively thicker and more diffuse until at a Reynolds number of 12 000 (Fig 2(d)) it extends over a distance of approximately 25 mm on the burner axis.

The effect of increasing Reynolds number on the detailed structure of the flames may be studied by reference to Figs 3 to 6. For each of the four flames these figures show the axial variation of mean velocity, the rms of velocity fluctuations, turbulence intensity and mean temperature, and also indicate the approximate time-averaged extent of the reaction zone along the burner axis.

At a Reynolds number of 2000 (Fig 3) the burner exit flow has a mean velocity of 3.3 m s^{-1}. The flow velocity increases slightly with distance from the burner port until at an axial distance of approximately 30 mm energy transferred from the reaction zone, located between 38 and 39 mm downstream, begins to heat up the unburnt gas. From this point, increases in temperature (see Fig 7) cause a rapid extension of the unburnt gases, and the flow accelerates through the reaction zone up to a peak velocity of 3.7 m s^{-1} just beyond the visible tip of this zone. Despite the laminar appearance of the flame, the burner exit flow is also seen to possess a fluctuating velocity component

Notation

A	Area of burner exit port
D	Diameter of burner exit port
f	Oscillation frequency
G	Volumetric flow rate of unburnt gas through burner
Re	Burner exit Reynolds number $\equiv (G/A)D/\nu$
t	Time
$\bar{T}$	Mean free stream temperature
Tu	Turbulence intensity $\equiv U_{rms}/\bar{U}$
U	Instantaneous velocity of free stream $\equiv \bar{U} + U'$
$\bar{U}$	Mean velocity
U'	Fluctuating velocity
U_{rms}	Root mean square of velocity fluctuations $\equiv \sqrt{(\overline{U'})^2}$
X	Downstream distance along flame centreline measured from burner port
Y	Cross-stream distance measured from flame centreline
ν	Kinematic viscosity of unburnt gas

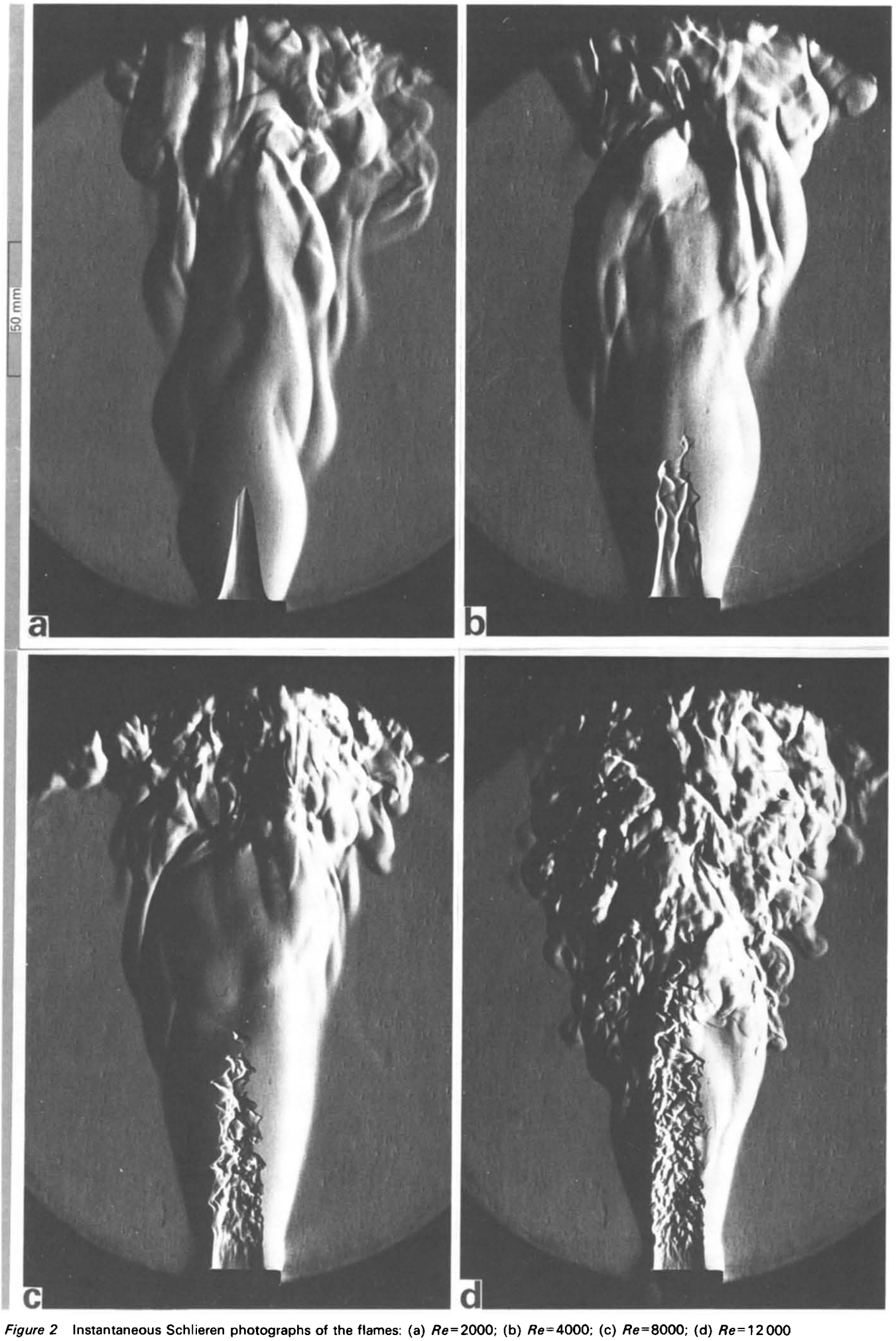

Figure 2 Instantaneous Schlieren photographs of the flames: (a) $Re=2000$; (b) $Re=4000$; (c) $Re=8000$; (d) $Re=12\,000$

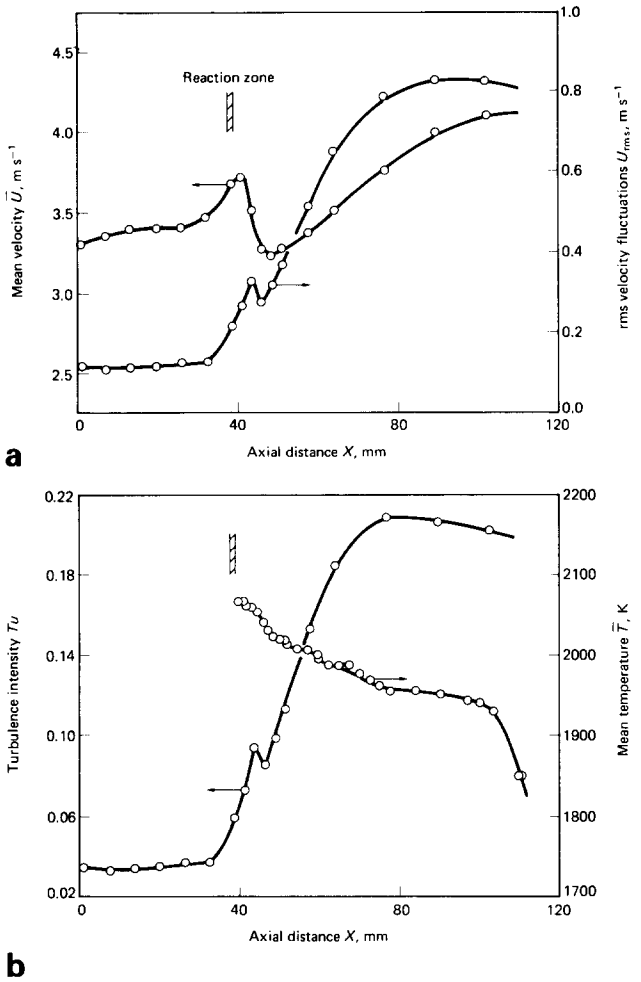

Figure 3 Axial variation of flame properties for the $Re = 2000$ flame: (a) mean velocity and rms of velocity fluctuations; (b) turbulence intensity and mean temperature

with an rms value of 0.12 m s^{-1}. This fluctuating velocity increases slightly until, at some distance from the burner port flow, acceleration causes a rapid increase up to a maximum value just downstream of the reaction zone.

From approximately 44 mm downstream both the mean and fluctuating velocity fall rapidly as flow expansion continues but the mean flow temperature begins to decrease. At 50 mm the mean velocity again increases because of buoyancy effects associated with the low density, high temperature burnt gases. The cause of the large and rapid increase in the rms of velocity fluctuations from 47 mm is the development of a series of large scale vortex rings in the shear layer of the flame which cause large scale motions in the overall flow. This aspect of the structure of the flames is discussed in detail in the following section.

The variation of turbulence intensity with axial distance through the $Re = 2000$ flame follows the same trends as those exhibited by the rms of velocity fluctuations. Also, following the rapid rise in temperature up to the flame reaction zone (Fig 7), mean temperature decays steadily with distance downstream until at approximately 100 mm the entrainment of ambient air results in a rapid decrease in temperature.

The reaction zone of the $Re = 4000$ flame (Fig 4) is located from 39 to 55 mm from the burner port. The burner exit flow has a mean velocity of 5.4 m s^{-1} which falls steadily with increasing axial distance until, at 30 mm downstream, the flow begins to accelerate. The mean velocity then increases up to a peak value at the tip of the reaction zone, after which point it decreases until, at 75 mm, downstream buoyancy effects again cause the mean velocity to increase. The fluctuating component of the burner exit flow shows a slight increase in its rms value until 30 mm downstream, but from this point follows the same trends as the mean velocity. The development of vortex rings in the shear layer of the flame is seen to affect the rms of velocity fluctuations on the flame axis from approximately 70 mm. Mean temperatures exhibit a steady rise and fall through the diffuse turbulent reaction zone, with a steady decrease in temperature occurring downstream of this zone until, at approximately 105 mm, air entrainment results in a more rapid decay.

In comparison with the $Re = 2000$ flame the properties of the $Re = 4000$ flame appear to be drawn out in the axial direction, with property changes being much less rapid than those encountered in the former flame. This effect continues with increasing burner exit Reynolds number as shown in Figs 5 and 6 for the $Re = 8000$ and 12 000 flames, respectively. Thus as Reynolds number increases, the reaction zone moves further downstream and becomes thicker and more diffuse in nature. Profiles of mean velocity become more drawn out but, because of the high Reynolds numbers of the flows, do not exhibit any effects of buoyancy. The variation of the rms of velocity fluctuations is similar to that of the $Re = 4000$ flame, although with increasing Reynolds number vortex rings in the shear layer of the flames begin to affect rms velocities at ever decreasing distances from the tip of the reaction zone. Mean axial temperatures reach a maximum at the visible tip of the reaction zone.

Radial profiles of mean temperature for the $Re = 2000$ and 12 000 flames are shown in Figs 7 and 8, respectively. In the $Re = 2000$ flame (Fig 7) the radial location of the reaction zone is seen to move progressively towards the flame axis with increasing distance from the burner exit, the data obtained at 40 mm downstream of the burner being just beyond the visible tip of the reaction zone on the flame axis. Radial temperatures are seen to increase rapidly through the reaction zone at the 15 and 30 mm positions, with temperature falling steadily with increasing radial distance after that zone. At positions beyond the location of the reaction zone on the flame axis, temperature fall off steadily with increasing radial distance. With increasing downstream distance, air entrainment also progressively

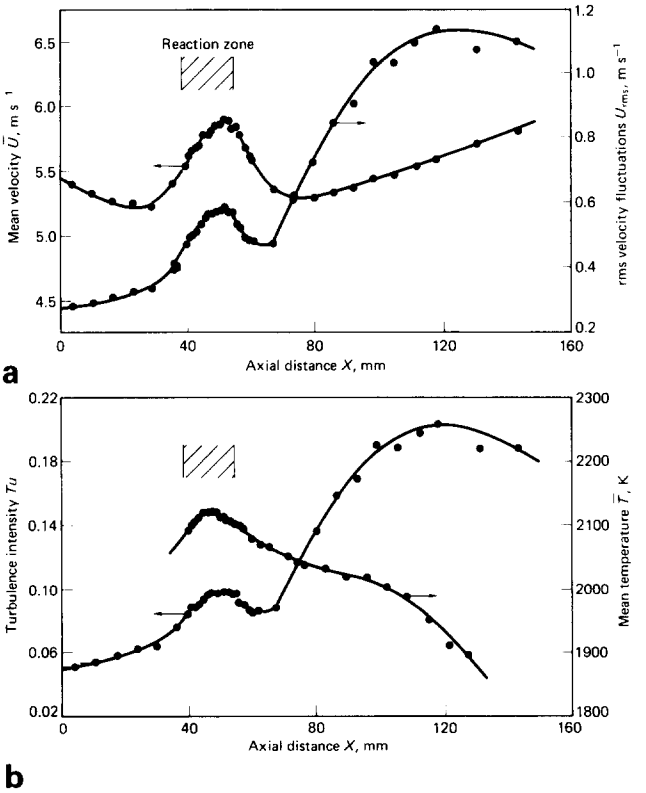

Figure 4 Axial variation of flame properties for the $Re = 4000$ flame: (a) mean velocity and rms of velocity fluctuations; (b) turbulence intensity and mean temperature

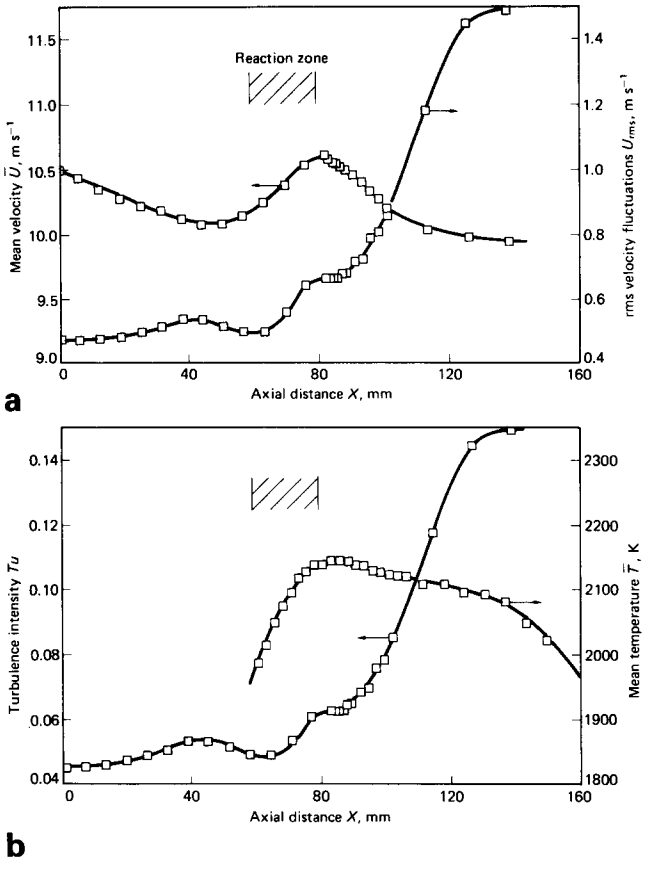

Figure 5 Axial variation of flame properties for the Re=8000 flame: (a) mean velocity and rms of velocity fluctuations; (b) turbulence intensity and mean temperature

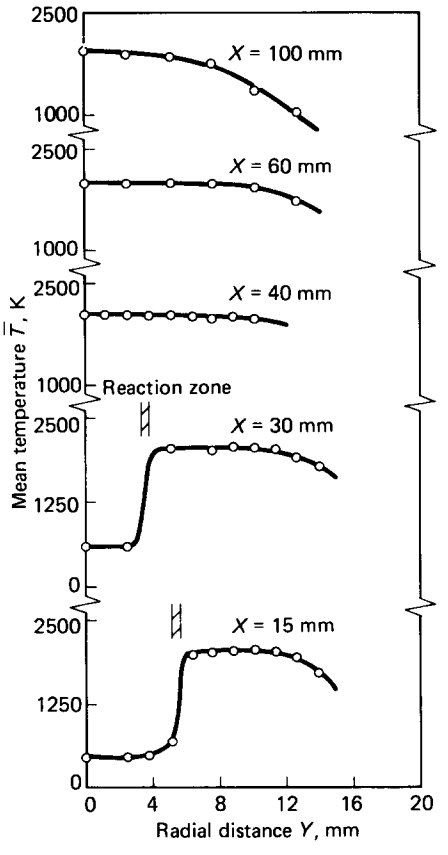

Figure 7 Radial variation of mean temperature for the Re=2000 flame

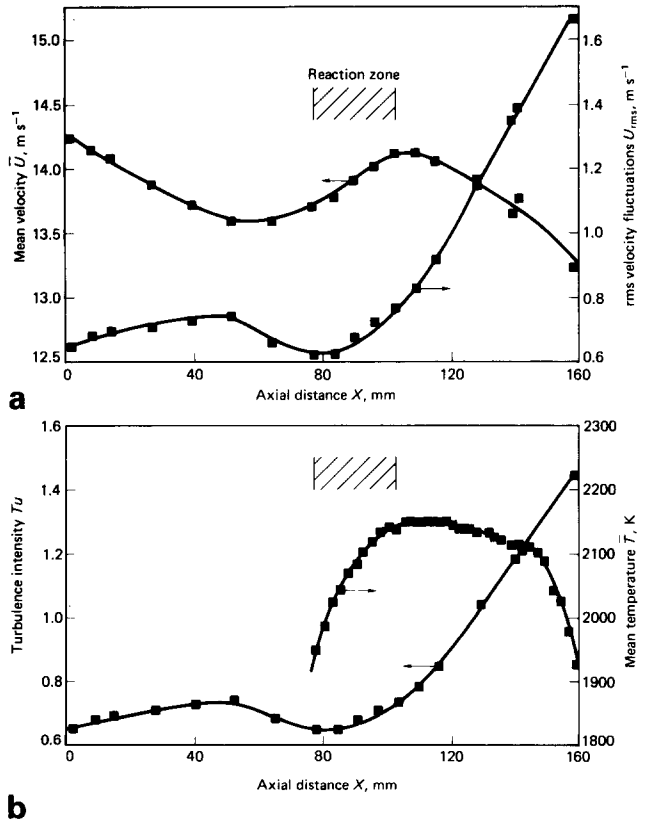

Figure 6 Axial variation of flame properties for the Re=12 000 flame: (a) mean velocity and rms of velocity fluctuations; (b) turbulence intensity and mean temperature

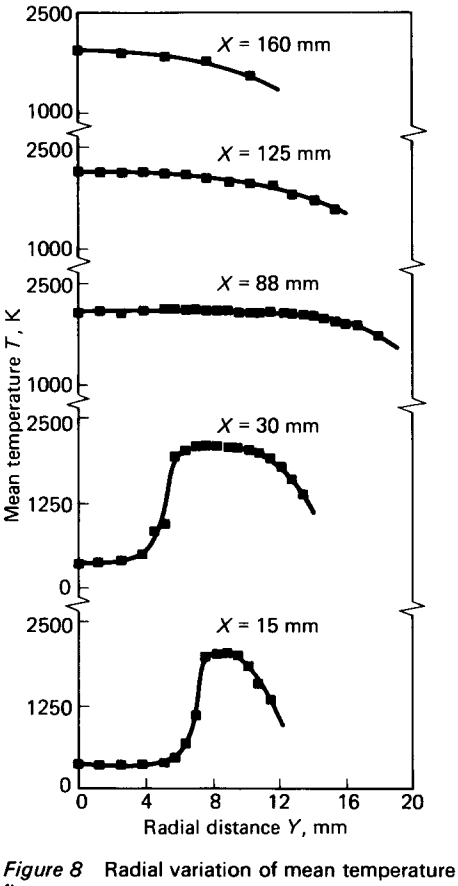

Figure 8 Radial variation of mean temperature for the Re=12 000 flame

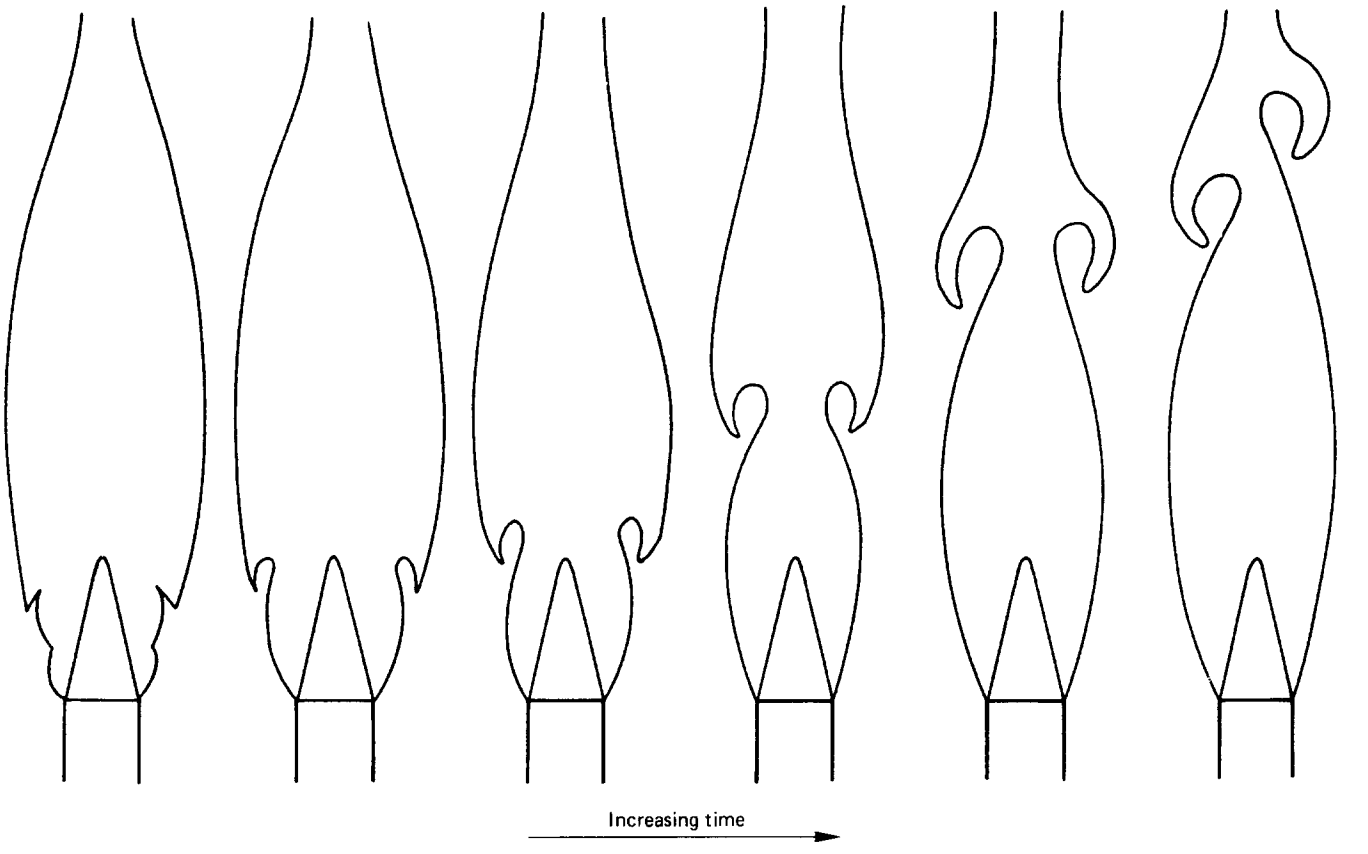

Figure 9 The development of a single flame oscillation

increases the rate of decay of radial temperature until at 100 mm downstream this effect leads to a rapid decrease in the flame centreline temperature (seen more clearly in Fig 3). Data for the $Re = 12\,000$ flame shown in Fig 8 are qualitatively similar to those of the $Re = 2000$ flame, although, at 15 and 30 mm downstream of the burner exit, radial temperature decays much more rapidly.

Radial measurements of mean velocity and the rms of velocity fluctuations were also obtained for the four flames. Similarly to the data shown in Figs 3 to 6, these measurements again demonstrated that at any given radial location the passage of unburnt gas through the flame front with increasing axial distance leads to increases in both the mean velocity and the rms of velocity fluctuations. Further details of these measurements may be found elsewhere[19].

Turbulent structure and low frequency oscillations

Measurements along the axes of the four flames revealed that large increases in the rms of velocity fluctuations occurred at some point just downstream of the reaction zone. This was attributed to the development of a series of large scale vortex rings in the shear layer of the flames, which cause large scale motions in the overall flow field.

Low frequency flame oscillations occurring at the boundary between the outer flame and surrounding air have been observed in both premixed and diffusion flames. This phenomenon is known as flame flicker, and the oscillations generally have a sinusoidal form. Studies of premixed flames[20-22] have shown that the frequency of oscillation is dependent on gas flow rate, the equivalence ratio of the unburnt gas, and burner design. In contrast, investigations of diffusion flames[23-25] have revealed that the oscillation frequency of these flames has a value between 10 and 11 Hz irrespective of the initial conditions of the flow.

The development of oscillations in the present flames was studied using a Schlieren-stroboscopic lamp apparatus, and also by means of a continuous light source Schlieren system which incorporated a light-beam chopper. The observed development of a single flame oscillation is illustrated in Fig 9. Instabilities in the shear layer close to the burner port lead to the development of a vortex ring which increases in scale as it is convected downstream by the main flow. With increasing distance from the burner port the vortex also migrates towards the axis of the flame, and eventually becomes circumferentially out of balance. Such vortices are clearly visible in the instantaneous Schlieren photographs of Fig 2.

The effect of these vortices on the instantaneous velocity along the centreline of the flames is illustrated in Figs 10 and 11, which show velocity–time data obtained in the $Re = 2000$ and 12 000 flames, respectively. It should be noted that the values for the mean velocity and rms of velocity fluctuations given in these figures do not coincide exactly with the data of Figs 3 and 6. This is because the data given in the latter figures are based on a time-averaging period of 3 s, whilst the data of Figs 10 and 11 are for the 0.2 s time period shown.

In the $Re = 2000$ flame (Fig 10) velocity fluctuations just downstream of the burner port are mainly high frequency, although some low amplitude, low frequency random velocity motions are in evidence. With increasing axial distance both the high frequency and random low frequency fluctuations increase in amplitude, until a position is reached at the approximate location of the flame reaction zone (38 to 39 mm downstream) where the low frequency fluctuations dominate. Beyond this position the instantaneous velocity is seen to oscillate at a regular low frequency with a relatively large amplitude. Superimposed on this low frequency fluctuation are the normal high frequency fluctuations attributable to turbulence generated by the burner pipe flow and augmented by the combustion process. With increasing axial distance the low frequency oscillation also increases in amplitude, until at 120 mm it starts to become irregular. Results for the $Re = 12\,000$ flame (Fig 11) are similar to those described above, although in this flame the low frequency oscillations are seen to be at a higher frequency over the whole flame length.

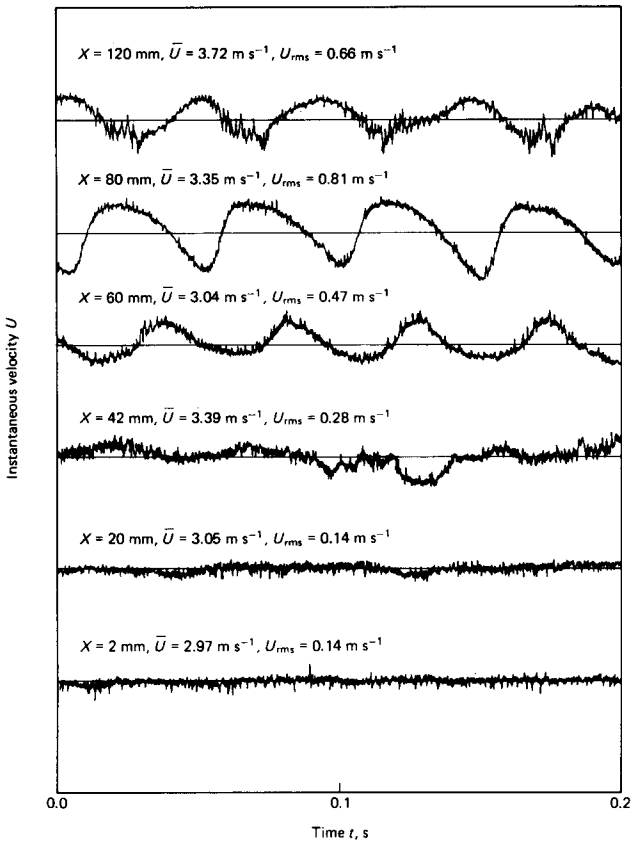

Figure 10 Velocity–time traces along the axis of the Re=2000 flame

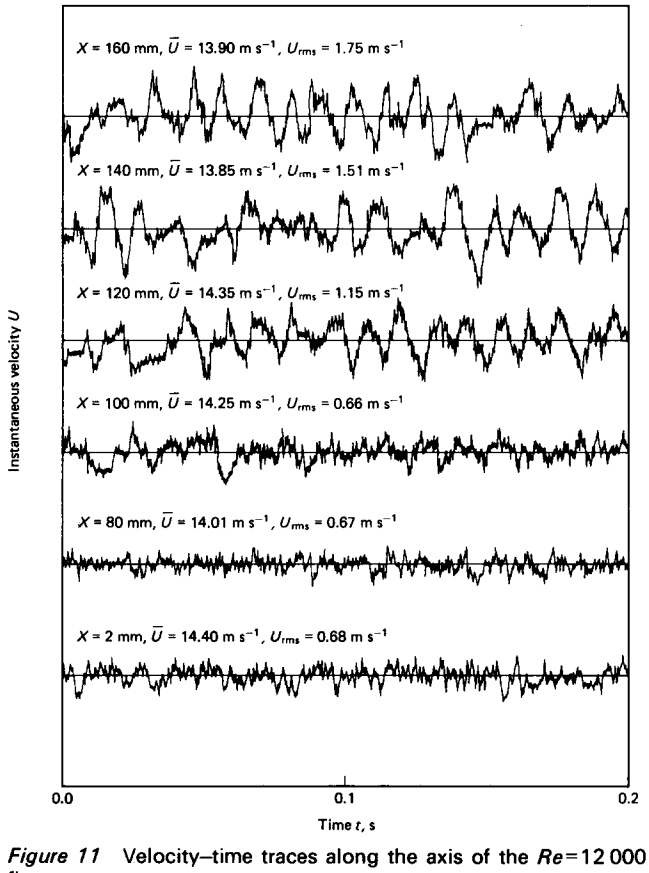

Figure 11 Velocity–time traces along the axis of the Re=12 000 flame

Fig 12 presents velocity–time data obtained at various radial locations in the Re=2000 flame. Results are given for two axial distances. At 30 mm downstream (Fig 12(a)) the reaction zone is located between approximately 3 and 4 mm from the flame centreline (see Fig 7), whilst the data at 42 mm (Fig 12(b)) are for an axial location just beyond the tip of the reaction zone. In Fig 12(a) instantaneous velocities measured at radial distances beyond the reaction zone show a regular low frequency oscillation which increases in amplitude with radial distance. Low frequency oscillations occur at radial positions inside the reacton zone, but these are more random in nature. With increasing axial distance (Fig 12(b)) the regular low frequency oscillation observed at a given radial distance is seen to increase in amplitude. Also, the effect of this regular oscillation extends closer to the flame centreline, and begins to cause regular oscillations on the centreline itself at approximately 60 mm downstream (Fig 10).

The oscillations occuring in the present flames are therefore of the same nature as those observed by Matsumoto *et al*[22] in turbulent premixed propane flames. The latter authors recognized that these oscillations stem from aerodynamic instabilities in the shear layer of a flame, as described by Durao and Whitelaw[24], and grow in the downstream direction whilst gradually extending towards the flame centreline. Thermal energy was recognized as being important to the development of the low frequency oscillations, the conversion of thermal energy to kinetic energy by the combustion process maintaining the large scale oscillations over the whole flame length. It was not, however, considered to be the direct cause of the oscillations since measured velocity and temperature fields near the reaction zone did not change when the oscillations were removed by means of a co-flowing air stream. This finding was verified in the present study by comparing measurements obtained in an oscillating flow with those taken when the oscillations were removed by placing a cylindrical wire gauze (50 mm in diameter and 40 mm long) concentric with the flame axis.

Matsumoto *et al*[22] also found an approximately linear relationship between the frequency of the oscillations and the burner exit Reynolds number for a given unburnt gas equivalence ratio, with oscillation frequency increasing over the Re=1100 to 1700 range examined. The variation of oscillation frequency with Reynolds number for the flames considered in the present study is shown in Fig 13, the frequencies having been obtained directly from flame centreline velocity–time traces. In this figure the trend established by four flames examined is seen to be confirmed by results obtained in Re=6000 and 10 000 flames.

From the above and previous results it may be concluded that turbulence along the flame centreline is not directly connected to the oscillation phenomenon until positions downstream of the reaction zone where vortices have migrated towards the flame axis and begun to break down into turbulent flow. Until such positions are reached the vortices merely pulse the mean velocity on the centreline of the flame and, from the axial profiles of mean temperature shown in Figs 3 to 6, do not appear to transfer significant amounts of entrained air from the extremities of the flame to its centreline. The latter conclusion is supported by the results of Matsumoto *et al*[22] where no difference between centreline mean temperatures measured in flows with and without oscillation was observed until far downstream of the reaction zone.

In terms of impingement heat transfer to bodies placed along the centreline of such flames, the rms velocity and turbulence intensity profiles presented in Figs 3 to 6 do not therefore characterize the flow turbulence that is responsible for augmenting the rate of heat transfer. Measurements of heat flux are made using bodies which are placed in a flame for relatively long periods of time when compared with the oscillation frequencies. In such situations convective heat flux is determined by the mean velocities and temperatures shown in Figs 3 to 6. The augmentation of heat transfer by free stream turbulence is caused by turbulence which is of a sufficiently

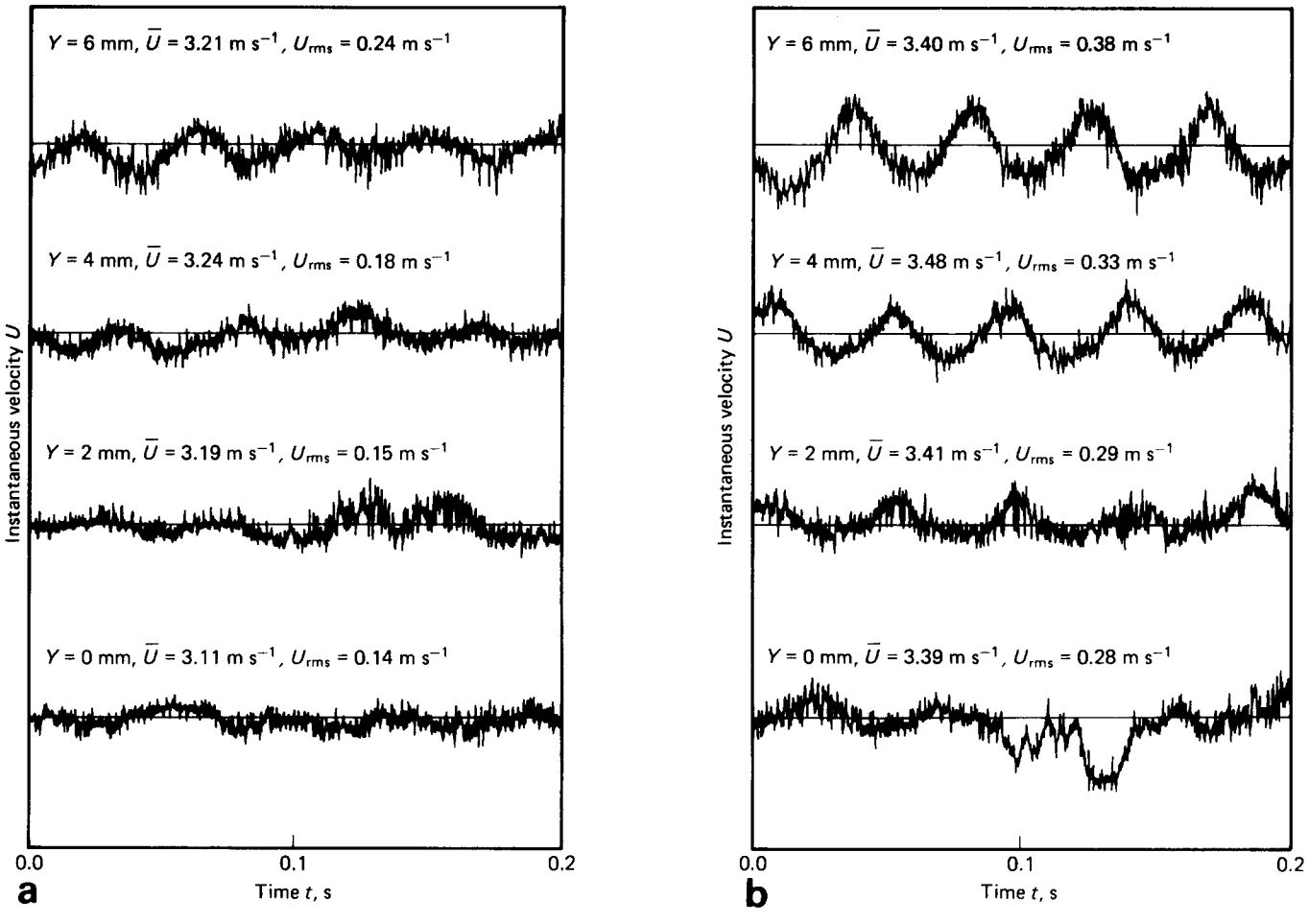

Figure 12 Radial velocity–time traces for the Re=2000 flame at axial distances of (a) 30 mm and (b) 42 mm

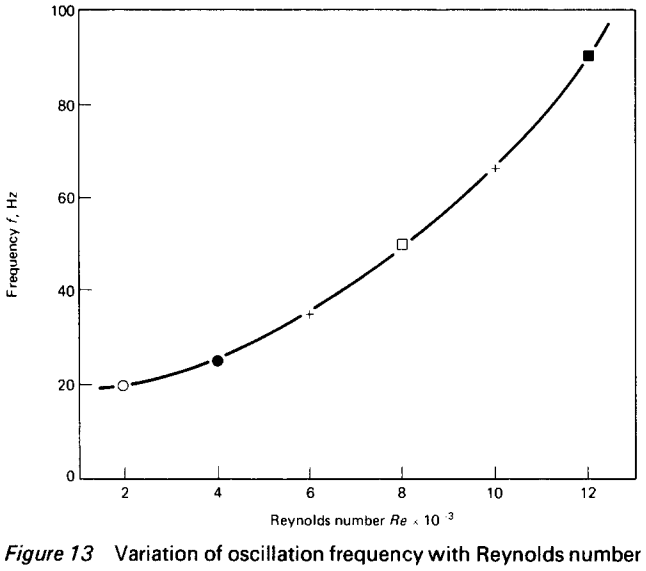

Figure 13 Variation of oscillation frequency with Reynolds number

small scale to be capable of penetrating the boundary layer around a body and to thereby affect its properties.

In order to provide values of free stream rms velocities and turbulence intensities more appropriate to the calculation of convective heat transfer rates, the data of Figs 3 to 6 were filtered to remove the low frequency fluctuations from the velocity signal and to allow the rms velocity of the high frequency components to be determined. This was achieved in two ways. Firstly, by using digital filtering which involved averaging the instantaneous velocity data over short periods of time to define an oscillating mean velocity, and then recalculating the velocity fluctuations about this mean. Secondly, an analogue high pass filter/amplifier unit with a suitable cut-off frequency was employed to filter instantaneous velocity data obtained directly from the LDA system.

Axial variations of turbulence intensity through the four stoichiometric flames obtained using the analogue filter are shown in Fig 14. For these flames, results derived using digital and analogue filtering were in closest agreement for an analogue filter cut-off frequency of 100 Hz. Comparison of the data of Fig 14 with those of Figs 3 to 6 shows that, for any particular flame, filtering leads to a slight decrease in measured turbulence intensities up to the flame reaction zone and large reductions thereafter.

Conclusions

As the first part of a study of convective heat transfer from impinging flames, the aerodynamic structure of four premixed flames was examined. These flames were of stoichiometric mixtures of methane and air with a Reynolds number range of 2000 to 12 000, extending from laminar to fully turbulent flow. Measurements of mean and rms velocities and mean temperatures were made within the flames, and instantaneous Schlieren photography and Schlieren-stroboscopic techniques were used to examine the visual appearance of the flames.

Instantaneous Schlieren photographs revealed that the flame reaction zone extends further downstream and becomes more ragged and diffuse with increasing Reynolds number. Measurements within the flames show that associated with this increase in the size of the reaction zone is a tendency for the

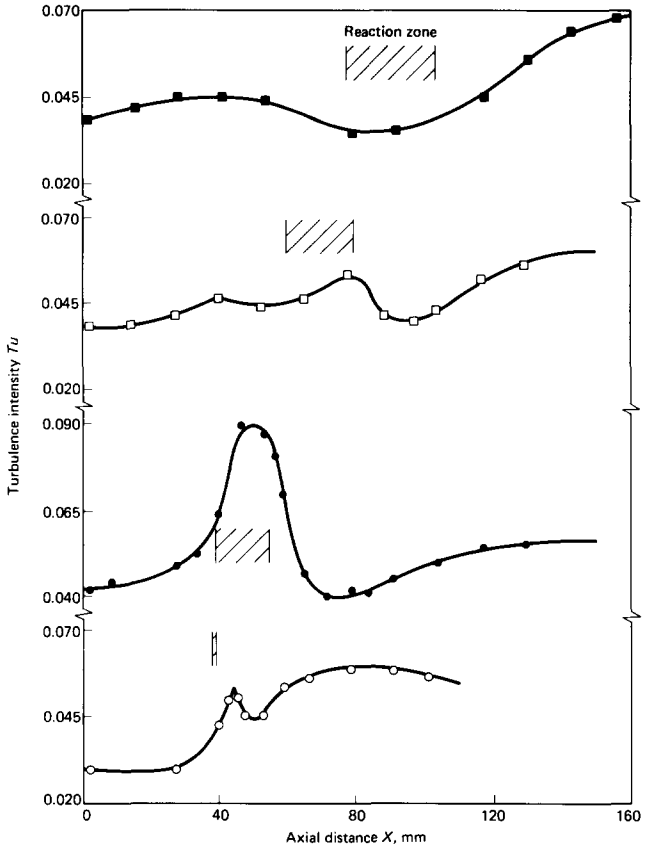

Figure 14 Axial variation of turbulence intensity obtained using an analogue filter with a 100 Hz cut-off (○ Re=2000, ● Re=4000, □ Re=8000, ■ Re=12 000)

properties of the flame to become drawn out in the downstream direction.

Schlieren-stroboscopic techniques revealed the existence of large scale vortex rings which originate in the shear layer of the flames, and grow in the downstream direction whilst gradually extending towards the flame centreline. This phenomenon gave rise to regular, low frequency oscillations in measured instantaneous velocities which in turn resulted in high rms velocities measured downstream of the flame reaction zone. Such high levels of rms velocity should not be interpreted as representing turbulence within a flame.

Acknowledgement

The authors would like to thank the British Gas Corporation for financing this project and for permission to publish.

References

1 Kilham, J. K. Energy transfer from flame gases to solids. *Third Symposium (International) on Combustion*, 1949, 733–740

2 Cookson, R. A. and Kilham, J. K. Energy transfer from hydrogen–air flames. *Ninth Symposium (International) on Combustion*, 1963, 257–263

3 Kilham, J. K. and Dunham, P. G. Energy transfer from carbon monoxide flames. *Eleventh Symposium (International) on Combustion*, 1966, 899–905

4 Kilham, J. K. and Purvis, M. R. I. Heat transfer from hydrocarbon–oxygen flames. *Combustion and Flame*, 1971, **16**, 47–54

5 Conolly, R. and Davies, R. M. A study of convective heat transfer from flames. *Int. J. Heat Mass Transfer*, 1972, **15**, 2155–2171

6 Fairweather, M., Kilham, J. K. and Nawaz, S. Stagnation point heat transfer from laminar, high temperature methane flames. *Int. J. Heat and Fluid Flow*, 1984, **5**, 21–27

7 Davies, R. M. Heat transfer measurements on electrically-boosted flames. *Tenth Symposium (International) on Combustion*, 1965, 755–763

8 Fells, I. and Harker, J. H. An investigation into heat transfer from unseeded propane–air flames augmented with D.C. electrical power. *Combustion and Flame*, 1968, 587–596

9 Buhr, E., Haupt, G. and Kremer, H. Heat transfer from impinging turbulent jet flames to plane surfaces. *European Symposium on Combustion*, 1973, 607–612

10 Horsley, M. E., Purvis, M. R. I. and Tariq, A. S. Convective heat transfer from laminar and turbulent premixed flames. *Proceedings of the Seventh International Heat Transfer Conference*, 1982, **3**, 409–415

11 Fairweather, M., Kilham, J. K. and Mohebi-Ashtiani, A. Stagnation point heat transfer from turbulent methane–air flames. *Combustion Science and Technology*, 1984, **35**, 225–238

12 Hargrave, G. K. and Kilham, J. K. The effect of turbulence intensity on convective heat transfer from premixed methane–air flames. *Proc. First UK National Conference on Heat Transfer, Inst. Chem. Engs. Symp. Series* No. 86, 1984, 1025–1034

13 Galloway, T. R. and Sage, B. H. Local and macroscopic transport from a 1.5-in. cylinder in a turbulent air stream. *A.I.Ch.E.J.*, 1967, **13**, 563–570

14 Galloway, T. R, and Sage, B. H. Thermal and material transfer from spheres, prediction of local transport. *Int. J. Heat Mass Transfer*, 1968, **11**, 539–549

15 Hargrave, G. K., Fairweather, M. and Kilham, J. K. Turbulence enhancement of stagnation point heat transfer on a body of revolution. *Int. J. Heat and Fluid Flow*, 1985, **6**, 91–98

16 Hargrave, G. K., Fairweather, M. and Kilham, J. K. Turbulence enhancement of stagnation point heat transfer on a circular cylinder. *Int. J. Heat and Fluid Flow* 1986, **7**, 89–95

17 Glass, M. and Kennedy, I. M. An improved seeding method for high temperature laser Doppler velocimetry. *Combustion and Flame*, 1977, **29**, 333–335

18 Fristrom, R. M. and Westenberg, A. A. *Flame Structure*, 1965, McGraw-Hill

19 Hargrave, G. K. A Study of Forced Convective Heat Transfer from Turbulent Flames. *PhD Thesis*, University of Leeds, 1984

20 Rutherford, A. G. and Fells, I. Oscillations in aerated Bunsen flames. *J. Inst. Fuel*, 1969, **42**, 26–28

21 Kimura, I. Stability of laminar-jet flames. *Tenth Symposium (International) on Combustion*, 1965, 1295–1300

22 Matsumoto, R., Nakajima, T., Kimoto, K., Noda, S. and Maeda, S. An experimental study on low frequency oscillation and flame-generated turbulence in premixed/diffusion flames. *Combustion Sci. and Technol.* 1982, **27**, 103–111

23 Toong, T.-Y., Salant, R. F., Stopford, J. M. and Anderson, G. Y. Mechanisms of combustion instability. *Tenth Symposium (International) on Combustion*, 1965, 1301–1313

24 Durao, D. F. G. and Whitelaw, J. H. Instantaneous velocity and temperature measurements in oscillating flames. *Proc. Roy. Soc.*, 1974, **A338**, 479–501

25 Grant, A. J. and Jones, J. M. Low-frequency diffusion flame oscillations. *Combustion and Flame*, 1975, **25**, 153–160